Received: 21 August 2023 | Revised: 8 November 2023 | Accepted: 20 December 2023

DOI: 10.1002/ijc.34867

RESEARCH ARTICLE

Molecular Cancer Biology

IJC INTERNATIONAL JOURNAL of CANCER | UICC

Neoadjuvant chemo- or chemo-radiation-therapy of pancreatic ductal adenocarcinoma differentially shift ECM composition, complement activation, energy metabolism and ribosomal proteins of the residual tumor mass

Maren N. Stillger[1,2] | Konrad Kurowski[1,3] | Peter Bronsert[1,3,4] | Eva Brombacher[2,5,6,7] | Clemens Kreutz[5] | Martin Werner[1,3] | Laura Tang[8] | Sylvia Timme-Bronsert[1] | Oliver Schilling[1,3]

[1]Faculty of Medicine, Institute for Surgical Pathology, Medical Center—University of Freiburg, University of Freiburg, Freiburg, Germany

[2]Faculty of Biology, University of Freiburg, Freiburg, Germany

[3]Faculty of Medicine, Core Facility for Histopathology and Digital Pathology, Medical Center—University of Freiburg, Freiburg, Germany

[4]German Cancer Consortium (DKTK) and German Cancer Research Center (DKFZ), Heidelberg, Germany

[5]Faculty of Medicine and Medical Center, Institute of Medical Biometry and Statistics, University of Freiburg, Freiburg, Germany

[6]Spemann Graduate School of Biology and Medicine (SGBM), University of Freiburg, Freiburg, Germany

[7]Centre for Integrative Biological Signaling Studies (CIBSS), University of Freiburg, Freiburg, Germany

[8]Department of Pathology, Memorial Sloan Kettering Cancer Center, New York, New York, USA

Correspondence
Oliver Schilling, Institute for Surgical Pathology, Universitätsklinikum Freiburg, Breisacher Strasse 115a, 79106 Freiburg, Germany.
Email: oliver.schilling@uniklinik-freiburg.de

Funding information
German Consortium for Translational Cancer Research project (Impro-Rec); investBW program, Grant/Award Number: BW1_1198/03; Deutsche Forschungsgemeinschaft, Grant/Award Numbers: 322977937, 405351425, 423813989, 431336276, 43198400, 441891347, 444936968, 446058856, 466359513; ERA PerMed program (BMBF), Grant/Award Numbers: 01KU1915A, 01KU1916; ERA TransCan program "PREDICO", Grant/Award Number:

Abstract

Pancreatic ductal adenocarcinoma (PDAC) is a highly lethal cancer, often diagnosed at stages that dis-qualify for surgical resection. Neoadjuvant therapies offer potential tumor regression and improved resectability. Although features of the tumor biology (e.g., molecular markers) may guide adjuvant therapy, biological alterations after neoadjuvant therapy remain largely unexplored. We performed mass spectrometry to characterize the proteomes of 67 PDAC resection specimens of patients who received either neoadjuvant chemo (NCT) or chemo-radiation (NCRT) therapy. We employed data-independent acquisition (DIA), yielding a proteome coverage in excess of 3500 proteins. Moreover, we successfully integrated two publicly available proteome datasets of treatment-naïve PDAC to unravel proteome alterations in response to neoadjuvant therapy, highlighting the feasibility of this approach. We found highly distinguishable proteome profiles. Treatment-naïve PDAC was characterized by

Abbreviations: CPTAC, Clinical Proteomic Tumor Analysis Consortium; DEA, differential expression analysis; DIA, data-independent acquisition; ECM, extracellular matrix; FDR, false discovery rate; FFPE, formalin fixed paraffin embedded; GPF, gas phase fractionation; LC–MS/MS, liquid chromatography tandem mass spectrometry; MSKCC, Memorial Sloan Kettering Cancer Center; NCRT, neoadjuvant chemo-radiation therapy; NCT, neoadjuvant chemotherapy; PCA, principal component analysis; PDAC, pancreatic ductal adenocarcinoma; PLS-DA, partial least-squares discriminant analysis; SAAV, single amino acid variant; TFA, trifluoracetic acid.

Laura Tang and Sylvia Timme-Bronsert have contributed equally to this study.

01KT2201; Mushett Family Foundation (MSKCC-Freiburg project)

enrichment of immunoglobulins, complement and extracellular matrix (ECM) proteins. Post-NCT and post-NCRT PDAC presented high abundance of ribosomal and metabolic proteins as compared to treatment-naïve PDAC. Further analyses on patient survival and protein expression identified treatment-specific prognostic candidates. We present the first proteomic characterization of the residual PDAC mass after NCT and NCRT, and potential protein candidate markers associated with overall survival. We conclude that residual PDAC exhibits fundamentally different proteome profiles as compared to treatment-naïve PDAC, influenced by the type of neoadjuvant treatment. These findings may impact adjuvant or targeted therapy options.

KEYWORDS

data-independent acquisition, mass spectrometry, neoadjuvant therapy, pancreatic ductal adenocarcinoma, proteogenomics

What's new?

Neoadjuvant treatments may have a tumor down-staging capacity in pancreatic ductal adenocarcinoma. However, the tumor biology of residual pancreatic ductal adenocarcinoma following neoadjuvant treatments remains largely unexplored. Here, using mass spectrometry-based proteomics and publicly accessible proteome datasets, the authors found fundamental proteome alterations between treatment-naïve pancreatic ductal adenocarcinoma and residual tumor mass after neoadjuvant chemo- or chemoradiation therapy. Treatment-naïve carcinoma was enriched in immunoglobulins and complement and extracellular matrix proteins, while post-treatment carcinoma presented high abundance of ribosomal and metabolic proteins. Further patient survival and protein expression analyses identified treatment-specific prognostic candidate markers.

1 | INTRODUCTION

Pancreatic ductal adenocarcinoma (PDAC) accounts for more than 90% of all pancreatic malignancies. With a 5-year survival rate below 10%,[1] PDAC is expected to emerge as the second leading cause of cancer-related deaths in the US by 2030.[2] Early stages are usually clinically silent leading to advanced tumor stages (52% stage IV) at the time of diagnosis.[1] Surgical resection is the exclusive curative treatment modality for PDAC, however merely 15%–20% of patients present with initially resectable tumors.[3] Following resection, adjuvant chemotherapy is beneficial and life-prolonging while the addition of radiation remained controversial.[4] Even in a resectable tumor stage (stage I–III) the long genetic evolution, tumor heterogeneity and the aggressive growth pattern result in high local recurrence rates.[5]

Recently, neoadjuvant therapy emerged as a strategy that allows early treatment of micrometastatic disease, and that may induce tumor regression.[6] Opinions vary whether neoadjuvant chemoradiation (NCRT) is superior to neoadjuvant chemotherapy (NCT) as patients' overall survival time does not improve significantly. A comparison of neoadjuvant treatment to "surgery first" treatment suggests that the overall survival time and incidence of resections are similar.[7,8] Nevertheless, it has been observed that neoadjuvant treatments have the capacity for tumor downstaging.

Poor responders to neoadjuvant treatments still face early disease recurrence and shortened overall survival,[9] highlighting the need for research on the tumor biology of residual PDAC following neoadjuvant treatment. Two recent studies used mass spectrometry-based proteomics to determine predictive biomarkers identifying poor responders for neoadjuvant-treated patients.[10,11]

Another mass spectrometry-based proteomic comparison showed depletion of glycolysis and fatty acid oxidation, and increased potential for stem cell-like properties of surviving cancer cells after NCT as compared to treatment-naïve PDAC.[12] Neoadjuvant chemotherapy (Folfirinox-based) treated tumors showed an enrichment of cytotoxic T cells and an anti-tumorigenic immune microenvironment.[13]

Here, we present the first proteomic characterization of residual PDAC after NCT or NCRT. We use data-independent acquisition (DIA) mass spectrometry (MS) to characterize and compare the proteomes of the residual tumors after both neoadjuvant therapies. In DIA, the mass spectrometer acquires MS/MS spectra independent of MS1 ion intensities. The protein coverage and quantification of DIA outperforms the standard data-dependent acquisition.

We analyzed formalin-fixed and paraffin-embedded (FFPE) tissue specimens. First, we compared the residual PDAC tumor after neoadjuvant treatment with treatment-naïve PDAC published in a study by Werner et al.[14] Afterwards, we performed a detailed comparison of both neoadjuvant treatments and correlated the proteome expression data with the survival time to identify potential prognostic candidate markers.

2 | METHODS

2.1 | Patient cohort and tissue processing

Patients that received neoadjuvant treatment were treated at the Memorial Sloan Kettering Cancer Center, NY, between 2012 and 2018. 67 PDAC patients received neoadjuvant treatment as described previously[15] and underwent either NCT or NCRT (Table S1). Resected tumor specimens were formalin-fixed and paraffin-embedded according to routine protocols. In addition, 14 treatment-naïve PDAC specimens that were collected and measured in a study by Werner et al,[14] were included into the differential protein expression analysis.

2.2 | LC–MS/MS sample preparation

For macrodissection, 10 µm thick PDAC specimens were deparaffinized and rehydrated using a decreasing xylol to ethanol series, and macrodissected by S. T.-B. Heat-induced antigen retrieval and protein extraction were performed as described earlier.[16] In short, proteins were extracted in an acid labile buffer (0.1% RapiGest in 1 M HEPES, pH 8.0) with the aid of sonication (Bioruptor, Diagenode), reduced with f. c. 5 mM DTT and alkylated with f. c. 15 mM iodacetamide. Proteins were double-digested with a protease mix consisting of trypsin (Sequencing Grade Modified Trypsin, Promega) and Lys-C (Lysyl Endopeptidase, MS Grade, Wako Pure Chemical Corporation) at 50°C for 2 h, and afterwards overnight at 37°C. Peptides were acidified with trifluoracetic acid and desalted using PreOmics cartridges (iST Kit, PreOmics).

2.3 | LC–MS/MS data-independent acquisition

All liquid chromatography-tandem MS (LC–MS/MS) data were acquired on a Q-Exactive Plus mass spectrometer (Thermo Scientific) coupled to an EASY-nLC 1000 UHPLC system (Thermo Scientific). The analytical column was self-packed with C18 silica beads (Reprosil Pur C18-AQ, $d = 3$ Å; Dr. Maisch HPLC GmbH) and coupled to a PepMap precolumn (C18, 75 µm diameter, 20 mm length; Thermo Scientific). A two-step linear gradient, increasing buffer B (0.1% formic acid in 80% acetonitrile, Fluka) from 8% to 43% over 90 min and from 43% to 65% over 20 min, was applied to separate peptides (800 ng per injection). For DIA, MS1 scans were performed at 70,000 resolution, an AGC target of 3e6, and a maximal injection time of 50 ms. The survey scan range was set between 385 and 1015 m/z. The MS2 isolation window size was set to 24 and 25 consecutive scans were performed in a stepwise overlapping manner. The resolution was set to 17,500, the AGC target to 1e6, the maximal injection time to 80 ms, and the stepped NCE to 25 and 30.

2.4 | Spectral library generation

To generate a cohort-specific spectral library, two pooled reference samples (8 samples each) were repeatedly measured using gas phase fractionation (GPF). Six measurements covering a fractionation window between 395 and 1005 m/z were conducted (100 m/z per measurement). The MS2 isolation window size was decreased to 4 m/z. DIA-NN 1.8[17] was used for library generation. Data files were converted to the software-specific .dia file format and analyzed against a human reference proteome (Uniprot: https://www.uniprot.org/ accessed June 14, 2021) containing 25,853 proteins. For library generation, the precursor FDR was set to 10%, deep learning-based spectra, RTs and IMs prediction were enabled. The peptide length was set between 7 and 30 amino acids, the precursor charge range between 1 and 4, the precursor m/z range between 400 and 1000, and the fragment ion m/z range between 200 and 1800. N-terminal methionine excision and cysteine carbamidomethylation were enabled. Trypsin was selected as the digestion protease, and two missed cleavages were allowed. The final library comprised 15,335 protein groups and 79,058 precursors.

2.5 | DIA sample analysis

Samples were analyzed using DIA-NN 1.8. Data files were converted to the .dia file format and analyzed against the cohort-specific library For sample analysis, the precursor FDR was set to 1%, and match between runs was enabled. All other parameters remained similar to the GPF analysis. One sample was removed from analysis after an initial analysis due to a low protein content (<3% of the average of all samples).

2.6 | Differential protein expression analysis

The statistical analyses were performed using R.[18] In order to integrate proteomic PDAC data from the Clinical Proteomic Tumor Analysis Consortium (CPTAC[19]) and from Werner et al[14] into a combined analysis, batch correction (Figure 1A) using the ComBat algorithm was applied.[20] Each dataset was defined as one individual batch. The expression matrix was inspected for missing values and filtered such that proteins that have at most 30% missingness per batch were retained. Expression data were median normalized, and submitted for differential protein analysis. For the in-depth comparison of NCT and NCRT, missing values were imputed via the ImpSecRob algorithm, which was suggested by DIMAR.[21] The partial-least squares discriminant analysis (PLS-DA) and principal component analysis (PCA) were performed using mixomics, and the differential expression analysis (DEA) using linear model for microarrays data (limma). The subsequent pathway enrichment analysis was performed using the topGO approach and the Fisher's exact test. Results were visualized using intrinsic R functions, EnhancedVolcano or ggplot2.

2.7 | Survival analysis

For the survival analysis, the lubridate, survival, survminer, cmprsk and CoxBoost packages were used. The survival time was calculated from

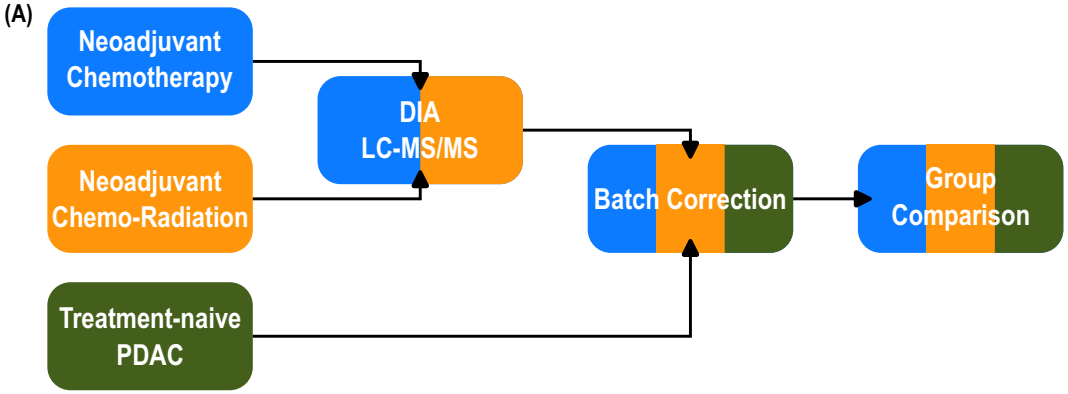

(B)

Variable		N	Hazard ratio		p
Age		66		1.00 (0.97, 1.04)	0.885
Sex	Male	35		Reference	
	Female	31		1.29 (0.65, 2.56)	0.464
Treatment	NCT	38		Reference	
	NCRT	28		0.95 (0.48, 1.88)	0.885
Differentiation	poor	10		Reference	
	poor to moderate	4		0.62 (0.12, 3.37)	0.584
	moderate	50		0.48 (0.18, 1.25)	0.130
	well	2		1.32 (0.21, 8.15)	0.767
Perineural Inv	No	13		Reference	
	Yes	53		1.02 (0.45, 2.29)	0.962
Vascular Inv	No	35		Reference	
	Suspected	3		3.50 (0.62, 19.75)	0.156
	Yes	28		3.24 (1.47, 7.13)	0.004
Recurrence	No	24		Reference	
	Yes	42		2.02 (0.98, 4.18)	0.058

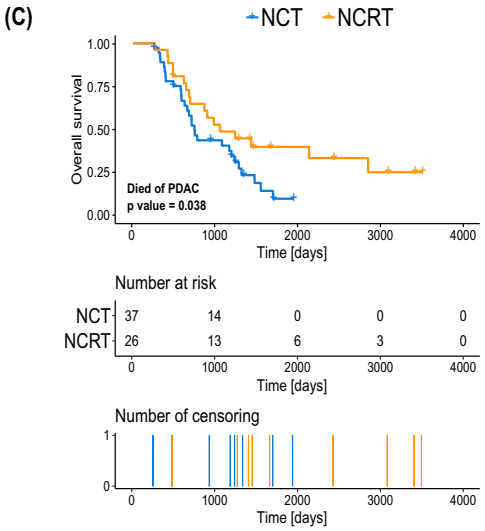

FIGURE 1 Experimental procedure and survival analysis (A) Schematic overview of the experimental and statistical procedure. (B) Cox proportional hazard model reveals increased hazard by vascular invasion ($p = .004$; multivariate cox proportional hazards model). (C) Overall survival of patients who deceased of PDAC differs between NCT and NCRT patients, assessed with a competing risk analysis ($p = .038$).

the day of diagnosis. A competing risk analysis was performed to examine the difference in the incidence of death by PDAC. A multivariate cox proportional hazards regression model was fitted to identify clinical parameters that affect the overall survival time. In order to identify potential prognostic candidate markers, the CoxBoost algorithm was applied. The penalty value and optimal number of boosting steps were determined using package-specific cross validation-based functions. To visualize the effect of a prognostic candidate marker on

overall survival, patients were divided into groups of high and low protein expression. For each protein, the cut point value based on the distribution of expression values was calculated using the survminer package. Patients were separated according to a given expression value: if they showed a value below/above the given cut point, they were assigned to the "low"/"high" expression group. Results were visualized using intrinsic functions from the packages, cowplot and forestmodel.

2.8 | Proteogenomic analysis

The proteogenomic analysis was performed according to a workflow by Pinter (https://github.com/npinter/ProteoGenDB). In short, the Galaxy environment (https://usegalaxy.eu/) was used to analyze paired-end RNA-Seq data from the Sequence Read Archive (SRA; https://www.ncbi.nlm.nih.gov/sra). The RNA-Seq reads (Table S2) were mapped to the human reference genome GRCh38. The resulting proteoform database (subFASTA) containing single amino acid variants (SAAVs) was processed locally with Python scripts to generate tryptic variant peptides (3596 entries) that were appended to the abovementioned human proteome reference database. This combined database was then used for the SAAV peptide search in DIA-NN 1.8. First, a spectral library was predicted (1,837,002 precursor and 7769 proteins) and then the LC–MS/MS samples were analyzed against this library.

3 | RESULTS AND DISCUSSION

3.1 | Overview of patient cohort

66 neoadjuvant treated patients were included in the following analyses as one patient was initially removed due to largely missing data points. All patients had been diagnosed with PDAC and received either NCT or NCRT before surgical resection (Table S1). In both therapy subgroups, patients received either folfirinox, folfox, gemcitabine or capecitabine-based chemotherapy regimens. They were treated at the Memorial Sloan Kettering Cancer Center, New York, USA, and were between 33 and 85 years old (median 66.5 years, mean 65.5 years). The median survival was 2.03 years. As detailed below, we further enriched the study by integrating publicly available proteomics data of treatment-naïve PDAC (Figure 1A).

3.2 | Vascular invasion is correlated to poor outcome following neoadjuvant treatment

We aimed to analyze whether clinical parameters affected the overall survival of the neoadjuvant treated patients. Therefore, we fitted a multivariate Cox proportional hazards model with the clinical patient data: treatment, differentiation, perineural and vascular invasion status, occurrence of recurrence, age and sex. As these parameters were not available for the treatment-naïve patients, they were excluded from this analysis. Individuals with an evident vascular invasion in the initial, treatment-naïve tumor ($n = 28$) presented a significantly increased hazard ratio of 3.24 ($p = 0.004$) compared to patients without a confirmed vascular invasion ($n = 35$; Figure 1B). Dismal overall survival was already reported to be accompanied by vascular invasion.[22] No other parameter affected survival.

3.3 | Cumulative incidence of death by PDAC decreases in NCRT patients as compared to NCT patients

We next compared the cumulative incidence of death by PDAC between NCT and NCRT patients using a competing risk analysis. In our cohort, NCRT patients had a significantly lower cumulative incidence of death from PDAC than NCT patients ($p = .038$; Figure 1C). The clinicopathological parameter might be cohort-specific and, therefore, differ from previous publications that report no difference. In addition, our observation is restricted to a group of patients with surgically removable tumors. In fact, in order to assess the superiority of either NCT or NCRT, it would be necessary to also include initially unresectable PDAC patients. For instance, about one-third of initially unresectable patients present with surgically removable tumors after NCT and comparable survival times to patients with initially resectable tumors[8,23]; however, data for NCRT patients was unavailable.

Overall, there is no consensus which neoadjuvant treatment modality is superior.[4,7,8,24] Chopra et al[7] showed that NCRT patients with surgically removable tumors demonstrated a longer disease-free survival than resectable NCT patients, although the overall survival was similar. In a number of studies, patients with initially resectable tumors who received neoadjuvant therapy presented similar progression-free and overall survival as compared to treatment-naïve patients with removable tumors.[4,7,8,24]

3.4 | Overview of proteome coverage

For the NCT and NCRT samples, the macro-dissected tissue volumes ranged between 0.08 and 3.02 mm^3. In a recent benchmarking study, we have shown that DIA-type proteomics is a powerful approach for characterizing the proteome biology of distinct tissues, even in the presence of inter-individual heterogeneity.[25] Hence, we have used DIA-type proteomics for the present study.

We identified 3592 proteins. Considerably more proteins were identified in the residual tumor mass after NCT as compared to NCRT (Figure 2A,B); however, Pearson correlation did not reveal coherence with the percentage of present stroma (Figure S1A,B). The proteome coverage remains below the Clinical Proteomic Tumor Analysis Consortium (CPTAC) study on PDAC proteomics,[26] but is substantially above the coverage reported by non-fractionated DDA-type proteomics.[27]

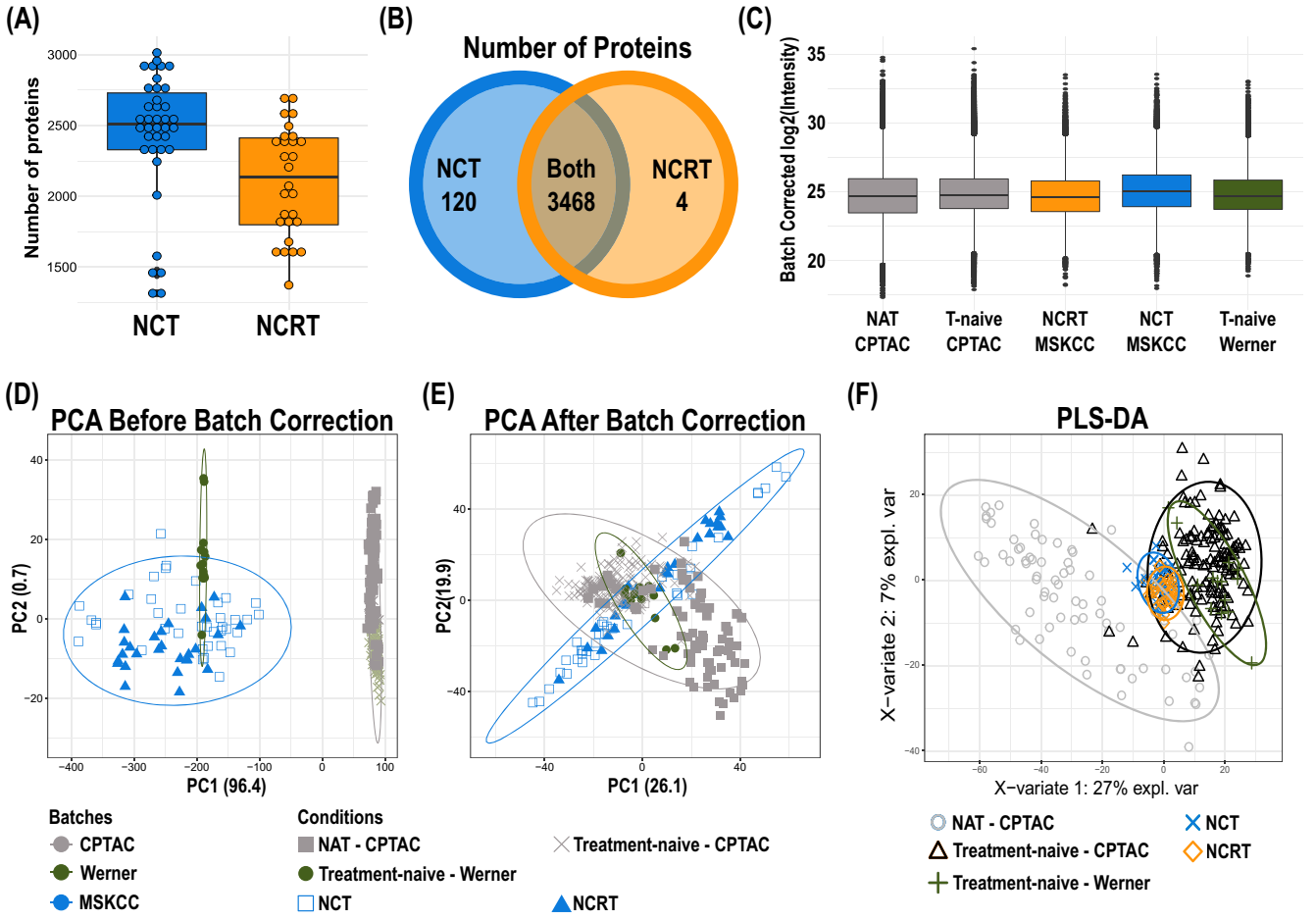

FIGURE 2 Data integration and protein quantification. (A) The number of identified proteins per neoadjuvant treatment (NCT = neoadjuvant chemotherapy, NRT = neoadjuvant chemo-radiation). (B) Overlap of all identified proteins. (C) Log2 protein expression in normal adjacent (NAT) pancreas from CPTAC, treatment-naïve PDAC from CPTAC, NCT and NCRT from the samples measured in this study (MSKCC = Memorial Sloan Kettering Cancer Center), and treatment-naïve PDAC from the Werner et al. study. (D-E) PCA before (D) and after (E) batch correction with ComBat. (F) Sparse PLS-DA after batch correction.

3.5 | Integration of publicly available proteomics data of treatment-naïve PDAC

We integrated our data with treatment-naïve PDAC and non-cancerous pancreas proteome profiles of the CPTAC,[19] and of a study by Werner et al[14] to enable a total of three proteomic comparisons (Figure 1A): (i) NCT vs treatment-naïve, (ii) NCRT vs treatment-naïve and (iii) NCT vs NCRT.

Among all three studies, 3356 proteins were commonly identified. The three datasets were integrated into one abundance matrix using the ComBat algorithm (Figure 2C–E).[20] Missingness was reduced to 30% per batch, yielding an expression matrix comprising 1709 proteins. Following median normalization, a sparse PLS-DA was performed (Figure 2F). The CPTAC PDAC and normal adjacent tissues (NAT) form two distinct clusters, albeit with partial overlap. Yet, all PDAC samples, regardless of the treatment and study, cluster into one group, proving their comparability.

Integrating CPTAC-derived NAT proteomes demonstrated that the data combination from various sites is practicable to gain further insights into different disease conditions. Despite measurements in different modes and on different mass spectrometers, data were combined using batch correction. Hence, these results encourage studying proteome profiles of diseases, where material is limited (e.g., rare cancers).

3.6 | Both NCT and NCRT yield enrichment of ribosomal and metabolic proteins as compared to treatment-naïve PDAC

The study conducted by Werner et al, and the measurements of the neoadjuvant treated samples both applied the DIA approach. PLS-DA showed a grouping of PDAC samples after batch correction and intensity normalization, demonstrating comparable proteome profiles (Figure 2F). Thus, we assume that the data by Werner et al and the neoadjuvant treated cohort are more comparable. In order to identify differentially regulated proteins, we performed differential expression analysis (DEA). In the following, we describe proteins as significantly

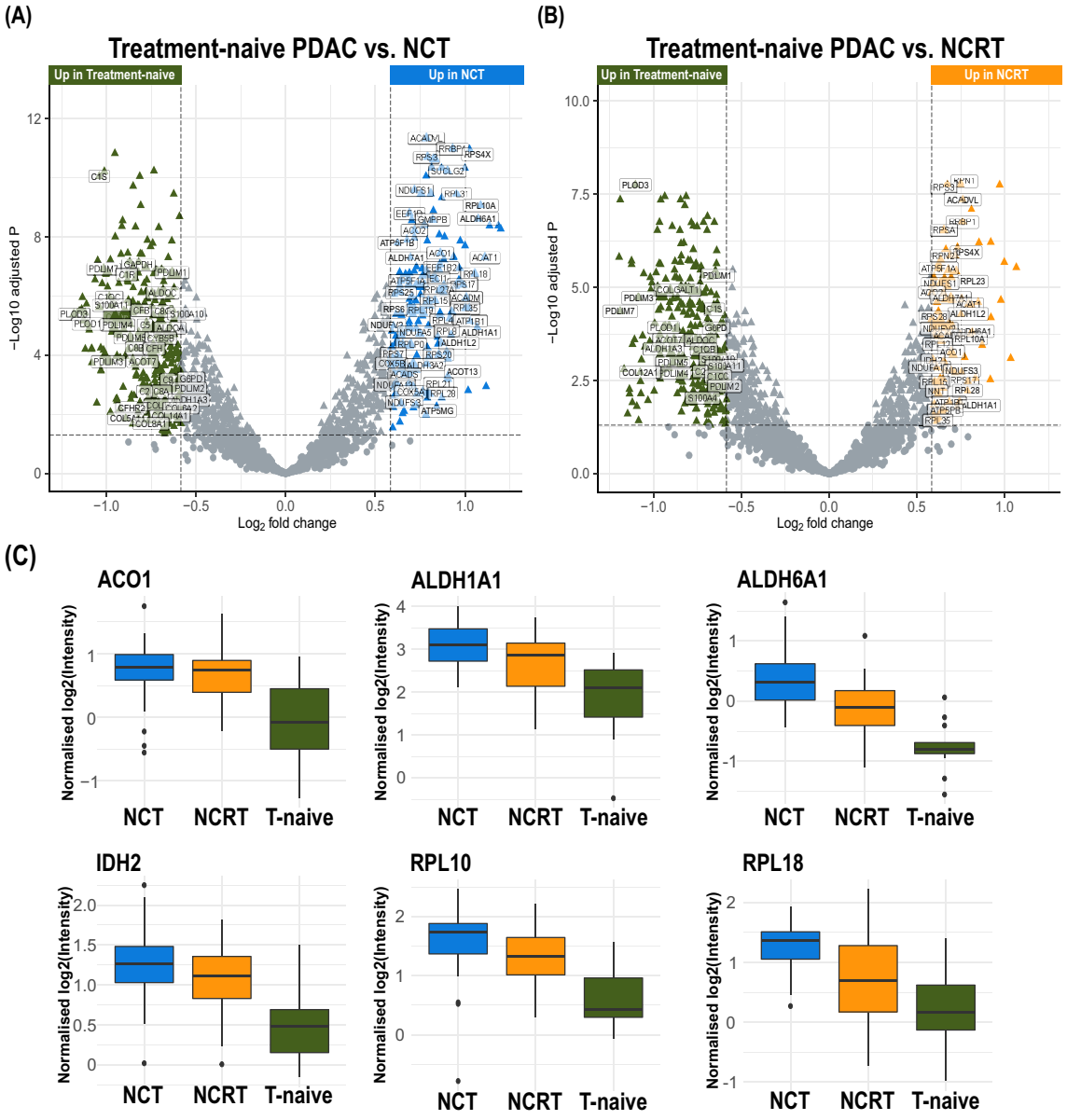

FIGURE 3 Proteome comparison of treatment-naïve PDAC and residual PDAC after neoadjuvant therapy. (A) Treatment-naïve PDAC vs NCT. (B) Treatment-naïve PDAC vs NCRT. Triangles indicate proteins with adjusted *p* values below .05. (C) Normalized and log2 transformed protein expression of selected significantly regulated proteins.

regulated, if their false discovery rate (FDR) is <0.05. If in addition, the fold change (log2[therapy/treatment-naïve]) is above 1.5, we call these proteins upregulated or below −1.5 downregulated, respectively.

As compared to treatment-naïve PDAC, post-NCT as well as post-NCRT tumors present significant proteomic changes (Figures 3A,B, S2A,B, Data S2 [Supplementary_Spreadsheet_1.xlsx] and Data S3 [Supplementary_Spreadsheet_2.xlsx]). For both, the sum of enriched proteins bears a fingerprint of ribosomal and metabolic proteins. Interestingly, metabolic changes were previously noticed in NCT (FOLFIRINOX)-treated as compared to treatment-naïve residual PDAC samples and organoids.[28] Amrutkar et al[12] reported a dysregulation of glycolysis, gluconeogenesis and the fatty acid oxidation between NCT and treatment-naïve PDAC. Together, these observations indicate a metabolic shift towards mitochondrial energy supply after neoadjuvant therapy.

Our results also corroborate previous findings on aldehyde dehydrogenases (ALDH) in PDAC.[12,27,29] We identified enrichment of ALDH1A1, ALDH1L2, ALDH3A2, ALDH6A1 and ALDH7A1 in both neoadjuvant treatments as compared to treatment-naïve PDAC (Figure 3C). Using MS, Amrutkar et al[12] also found an increased ALDH1A1 expression in NCT as compared to treatment-naïve PDAC. In a previous study, Oria et al[27] reported that ALDH1A1 inhibition sensitizes PDAC cells to gemcitabine, radiation and chemoradiation

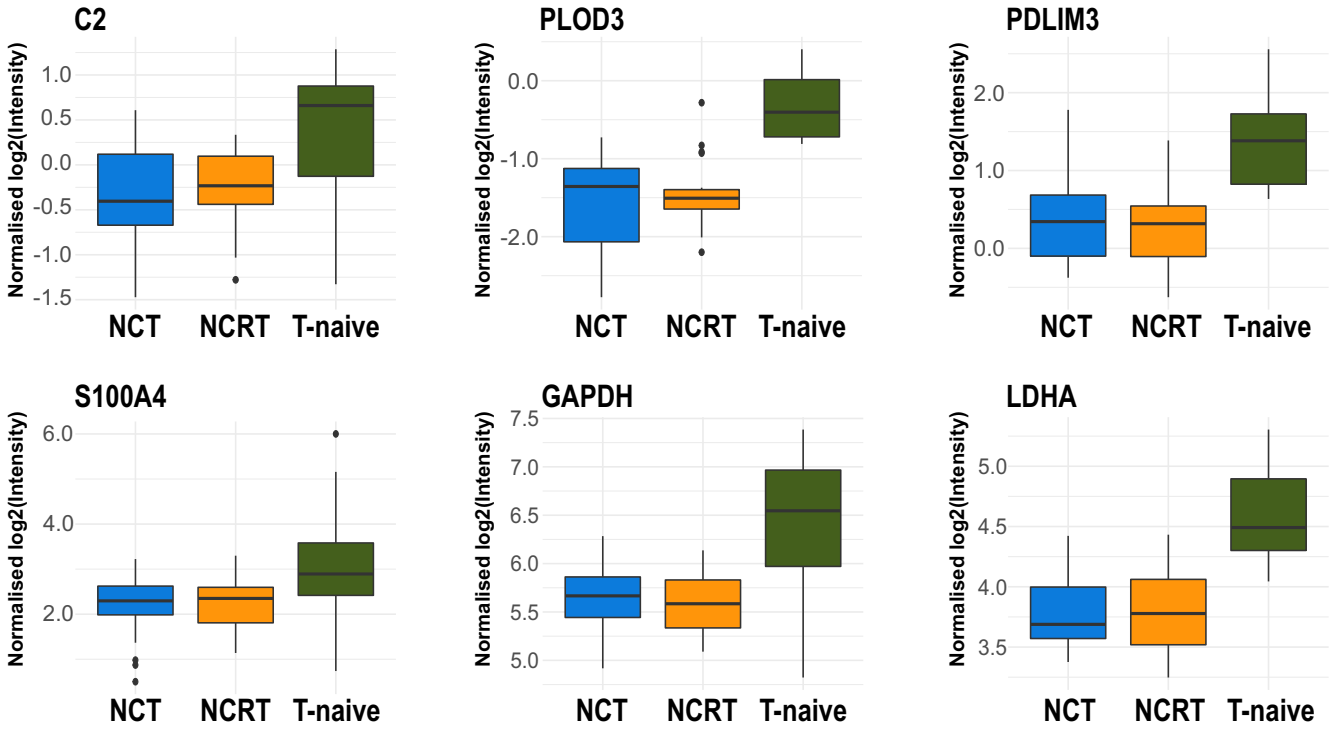

FIGURE 4 Protein expression in treatment-naïve PDAC and post neoadjuvant therapy PDAC. Normalized and log2 transformed protein expression of selected significantly regulated proteins.

in vitro. This suggests that the increased ALDH abundance may contribute to therapy resistance in the context of neoadjuvant therapy.

3.7 | Both NCT and NCRT yield depletion of glycolytic, ECM, S100 and PDLIM proteins as compared to treatment-naïve PDAC

For both, NCT and NCRT, we noticed depletion of glycolysis associated proteins (GAPDH, LDHA), ECM proteins such as PLOD1 and PLOD3 involved in collagen modification, immune proteins such as complement C1 and C2, CD47, cytoskeletal scaffold proteins (PDLIM family) and S100 proteins (Figure 4) as compared to treatment-naïve PDAC.

Our findings corroborate a previous global transcriptome profiling, in which the authors also found depletion of the complement system (decreased C3 and C4BPB expression) in NCT-treated residual PDAC as compared to treatment-naïve PDAC.[28] In our data, this change was more pronounced in NCT than in NCRT as compared to treatment-naïve PDAC.

In addition, our results corroborate a previous MS-based profiling that noticed decreased protein expression of PLOD3, GAPDH and LDHA in NCT as compared to treatment-naïve PDAC.[12] A number of publications associated S100 proteins with tumor proliferation and poor survival in PDAC.[30–32] Depletion of proteins, which are often found overexpressed or associated with a dismal survival in PDAC, may generally indicate efficacy of neoadjuvant therapy and elucidate proteins, which are worth being studied as diagnostic biomarker.

3.8 | NCT and NCRT yield distinct features of residual PDAC proteomes

We progressed to compare the proteomes of both neoadjuvant therapies in more detail. We retained proteins with at most 30% missingness per group (NCT or NCRT). To counter batch effects arising from sample preparation, we used ComBat[20] (Figure S3A). Following median normalization, missing values were imputed using the impSecRob algorithm. Using DIMAR,[21] we evaluated the optimal imputation algorithm. Finally, 2040 proteins were included for further analyses.

Sparse PLS-DA separated NCT from NCRT based on their expression profiles (Figure 5A). NCRT and NCT patients separated into two distinct groups, albeit two NCRT samples crossed the separation border (CR19 and CR26). Unsupervised hierarchical clustering (Euclidean distance and complete-linkage clustering), did not present clustering according to treatment or within one treatment group (Figure S4).

3.9 | Patient-specific factors impact the distinct proteome biology in residual PDAC

We performed differential expression analysis (DEA) in order to identify dysregulated proteins between both neoadjuvant

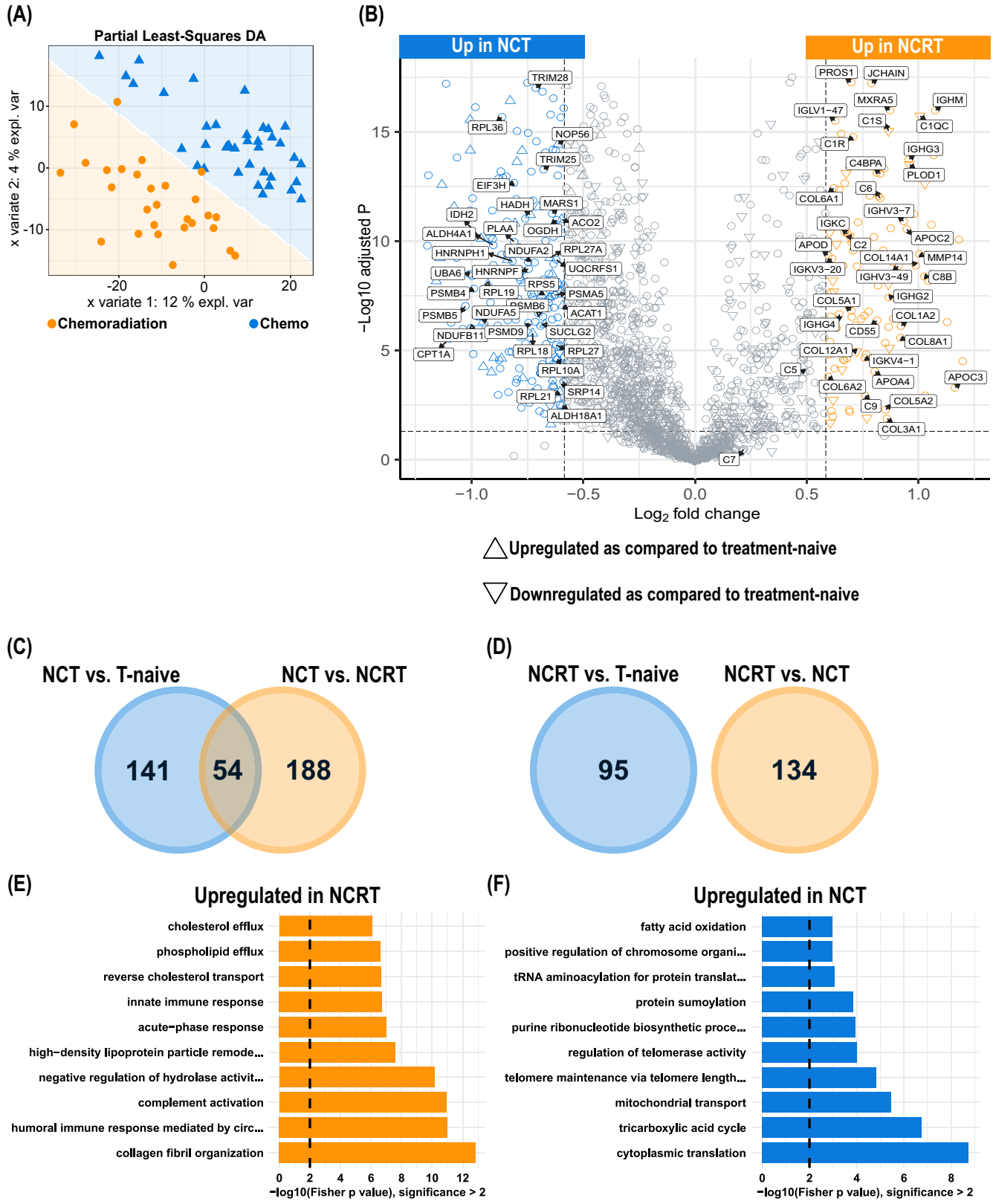

FIGURE 5 Differentially regulated proteins between NCT (n = 38) and NCRT (n = 28). (A) Partial least-squares discriminant analysis (PLS-DA) indicates separation of the proteomes. (B) Volcano plot showing the log2 fold change and -log10 of the adjusted *p* values of all 2040 proteins included in the DEA model. Differentially regulated proteins: 134 proteins enriched in NCRT (orange) and 242 proteins enriched in NCT (blue); 1664 proteins remained unchanged. (C, D) Overlap of proteins enriched in (C) NCT and (D) NCRT as compared to each other and treatment-naïve PDAC. (E, F) Pathway enrichment analysis using the topGO approach: (E) Pathways enriched in NCRT and (F) NCT.

therapies. To examine, whether clinicopathological parameters affect the differential protein expression, we included them as covariates to the linear model. Since under the null hypothesis (no impact) the *p* value distribution from the linear model analysis of all proteins is expected to be uniform, the observed shift of the distribution towards zero and the substantial proportion of *p* values below .05 suggest a strong global impact of those variables on the proteome (Figure S5A–E).

3.10 | NCT yields enrichment of ribosomal and metabolic proteins as compared to NCRT

The ribosomal and metabolic fingerprint appears to be more pronounced in NCT as compared to NCRT. Proteins overrepresented in NCT vs NCRT include proteins of translation, ribosomal proteins, proteasome components and proteins comprising the metabolic energy supply (Figure 5B,C and Data S4 [Supplementary_Spreadsheet_3.xlsx]). We detected enrichment of 60S and 40S ribosomal proteins (RPL3, RPL8, RPL10A, RPL11, RPL17, RPL18, RPL19, RPL21, RPL27, RPL27A, RPL34, RPL36, RPS5), essential for ribosome stability.[33] HNRNPF, HNRNPH1, EIF3H, EIF4G and MARS1, which regulate mRNA splicing, initiate and execute translation are also enriched in NCT vs NCRT. We also detected increased abundance of signal recognition particles (SRP14, SRP68 and SR72), which guide proteins to the endoplasmic reticulum. The proteasome subunits PSMB4, PSMA5, PSMB5 and PSMB6, the chaperone PSMD9, and the adaptor and scaffold protein ECM29 are enriched in NCT vs NCRT. In accordance with this, UBA1, UBA6, HECTD3, PLAA, TRIM25 and TRIM28, which promote protein ubiquitination for proteasomal degradation, are significantly enriched in NCT vs NCRT.

PDAC typically exhibits the Warburg effect coupled with heightened glucose consumption, wherein tumor cells favor lactate production from pyruvate for ATP generation.[34] In accordance, Werner et al observed a depletion of mitochondrial metabolic proteins (IDH2, ACO1, SUCLG2), and upregulation of GAPDH, reminiscent of the Warburg effect, in treatment-naïve PDAC as compared to non-cancerous pancreas. In this study, NCT displayed LDHA and GAPDH depletion as compared to treatment-naïve PDAC (Figure 5B), and increased expression of proteins of the TCA cycle and respiratory chain, shifting towards a mitochondrial energy supply. This shift is suggested to be more pronounced in post-NCT than post-NCRT tumors as executors of the TCA cycle such as IDH2, OGDH, ACO2 and SUCLG2 are enriched in NCT vs NCRT. Key components of the fatty acid oxidation such as ACADM, ACAT1, CPT1A and HADH are also enriched, along with mitochondrial proteins, for example, complexes I (NDUFA2, NDUFA5, NDUFB11), III (UQCRFS1) and IV (COX5B, COX6B1) of the respiratory chain, and the ATP synthase ATP5MG (oxidative phosphorylation) in NCT vs NCRT. Enrichment analysis confirmed an overrepresentation of ribosomal and metabolic proteins (Figure 5F).

3.11 | NCRT yields enrichment of ECM proteins and complement activation as compared to NCT

Proteins that are increased in NCRT as compared to NCT present a strong fingerprint for apolipoproteins (A1, A4, C2, C3, ApoD, ApoL-II), ECM proteins, the complement system (C1, C2, C4-B, C6, C8-B, C9 and C4BPA), and immunoglobulins (heavy constants and variables) (Figure 5B,D and Data S4 [Supplementary_Spreadsheet_3.xlsx]). The ECM proteins include 11 collagens (COL1A1, COL1A2, COL3A1, COL5A1, COL5A2, COL6A1, COL6A2, COL8A1, COL11A1, COL12A1, COL14A1), PLOD1, MMP14, biglycan PGS1 and MXRA5 (Figure 5A). Again, the topGO enrichment analysis confirmed an overrepresentation of proteins involved in collagen fibril organization, complement activation and innate immune response in NCRT as compared to NCT (Figure 5E).

Our findings are largely in line with a recent gene expression- and immunohistochemistry-based study that reported an altered collagen pattern after neoadjuvant therapy, including depletion of collagen types I, III, IV and V; however, 20 NCT and 5 NCRT patients were analysed together. In vitro analysis indicated that the collagen depletion might contribute to tumor shrinkage.[35] In addition, collagen type I and MMP14 are reported to promote gemcitabine resistance in PDAC and are often found overexpressed in PDAC.[36,37] In our proteomic comparison, we showed that collagens are enriched in NCRT as compared to NCT. With the exception of COL12A1, collagen expression remained unchanged between NCRT and treatment-naïve PDAC. In contrast with these findings, a RNA-Seq profiling study encompassed enriched ECM organization and collagen formation in NCT as compared to treatment-naïve PDAC.[38] A second gene expression study reported increased collagen transcription in NCRT-treated samples as compared to biopsies taken before the intended neoadjuvant therapy.[39] Taken together, this is an area of ongoing research, especially since a fibrotic ECM rich in collagens is a hallmark of PDAC, promoting tumor progression and chemoresistance.[36] A therapy-induced depletion of collagens may contribute to better therapy response and benefit adjuvant therapy. In addition, these findings also highlight the importance of the distinct analysis of different types of neoadjuvant therapy as altered tumor biology may guide adjuvant therapy.

A report on gene expression-based immunologic profiling suggests profound immunologic alterations—including the complement system—after NCRT,[40] while our study suggests complement activation particularly in NCRT vs NCT. While inhibitors of the complement system are entering into clinical practice, findings vary as to the function of the complement pathway in cancer,[41,42] ranging from anti-tumor defense to tumor promotion.[42,43]

Further, we observed that CD163 (macrophage polarization marker) is more abundant ($p_{adjusted} = .04$, fold change $= -0.31$) in NCRT as compared to NCT (Figure S3B), suggesting a possible shift towards M2 polarization; in line with a report by Dias Costa et al.[13] Both the complement and macrophage footprint highlight a differential impact of NCRT vs NCT with regard to the PDAC immune microenvironment.

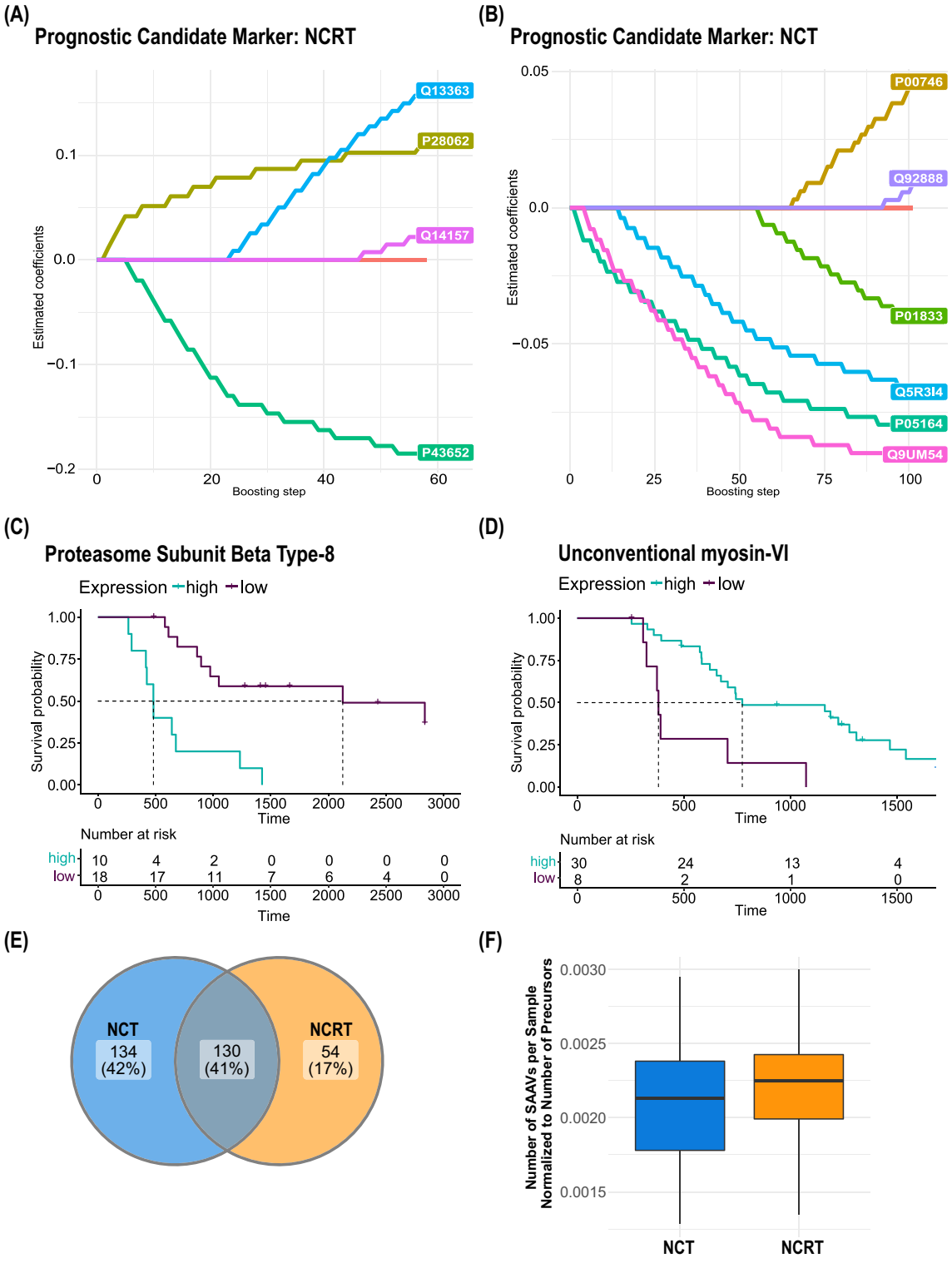

FIGURE 6 Prognostic proteins that are associated with patient survival and single amino acid variant (SAAV) analysis. CoxBoost coefficients deviating from zero indicate prognostic proteins. The earlier the coefficients deviate from zero, the higher their impact. Coefficients <0 positively affect survival, coefficients >0 have a negative impact. (A) Prognostic proteins in NCRT (n = 28), and (B) in NCT (n = 38). (C) Overall survival probability of NCRT patients with high (turquoise) and low (purple) PSMB8 expression. (D) Overall survival probability of NCT patients with high (turquoise) and low (purple) MYO6 expression. (E) Number and overlap of identified SAVVs in NCT and NCRT. (F) Number of SAAVs per sample normalized to the number of precursors per sample in NCT and NCRT.

3.12 | The residual PDAC proteomes after NCRT or NCT feature different prognostic candidates

We used the CoxBoost algorithm to identify prognostically relevant proteins. Clinical parameters (age, sex, differentiation, vascular invasion and perineural invasion status) were included to the model as covariates. Since both neoadjuvant groups showed huge differences in their proteome profiles, we decided to analyze the prognostic potential of the proteome profiles in both groups independently.

In NCRT, two proteins were associated with the survival time of patients (Table S3 and Figure 6A). PSMB8 (P28062)—a componenent of the immunoproteasome—segregates within the first 30 boosting steps and reaches estimated CoxBoost coefficients >0.04, which is indicative of proteins where elevated levels are accompanied with a dismal overall survival (Figure 6C). In contrast, AFM (P43652), a plasma protein, was associated with a favorable overall survival (CoxBoost coefficients < −0.04) (Figure S6A). In ovarian cancer, high AFM levels are indicative of a favorable outcome.[44] In gastric cancer, low AFM serum levels were proposed as a predictive early disease marker.[45] PSMB8 was not associated with PDAC survival so far, yet, its deletion in acute pancreatitis results in persistent pancreatic damage.[46]

In NCT, two proteins were associated with a favorable overall survival (Table S3 and Figure 6B). MYO6 (Q9UM54) (Figure 6D) and MPO (P05164) (Figure S6B) segregate within the first 30 boosting steps and reach estimated CoxBoost coefficients < −0.04. MYO6 upregulation was observed in prostate[47] and ovarian cancer,[48] however, it was not described to affect survival so far. MPO is part of the innate immune system and associated with a favorable prognosis in breast and colorectal cancer.[49,50]

Our proteome data suggests different prognostic candidate markers in both therapeutic subgroups, further underlining differential proteome biology. Yet these proteins do not map to the hallmark proteome features of either treatment group.

3.13 | Proteogenomic analysis and identification of single amino acid variants

Proteogenomic analyses combine proteomic and genomic and/or transcriptomic data to identify potential sequence variants, such as single amino acid variants (SAAVs), or copy number variations. The proteogenomic landscape of PDAC has been recently published as part of the CPTAC.[26] In our study, we used publicly accessible transcriptomic PDAC data (Table S2) in order to identify potential SAAVs on the proteome level. The transcriptomic data were used to search for mutations that lead to SAAVs in peptide sequences. In total, we identified 319 SAAVs among all neoadjuvant treated patient samples. 264 SAAVs were identified in NCT (median SAAVs per sample = 37), 184 SAAVs in NCRT (median SAAVs per sample = 29) (Figure 6E). Since we identified a higher number of peptides in NCT, we assessed the abundance of SAAVs in relation to the number of peptides per sample from the same search (Figure 6F). We did not detect a significant difference in the abundance of SAAVs (Welch two sample *t* test: *p* value = .3775). Off note, we want to mention that the SAAVs we identified may also represent potential benign mutations and naturally occurring allele variants. Among the 13 most frequent SAAVs (present in at least 50% of samples; Table S4), six were already annotated as benign SAAVs in the ClinVar database (https://www.ncbi.nlm.nih.gov/clinvar/). In order to identify the mutational burden for each patient further experiments would be required, which is beyond the scope of this study.

4 | CONCLUSION

In the present study, we investigated the proteome biology of the residual PDAC tumor mass after NCT or NCRT. We integrated published proteome data of treatment-naïve PDAC into our analysis to reveal proteome changes induced by neoadjuvant therapy. We conclude that the proteome profiles differ fundamentally between neoadjuvant treated residual tumors and treatment-naïve PDAC. ECM, immunoglobulin and complement proteins are overrepresented in treatment-naïve PDAC. Post-NCT and post-NCRT tumors share enrichment of ribosomal and mitochondrial proteins, and depletion of glycolytic proteins as compared to treatment-naïve PDAC. Notably, this enrichment and depletion are more pronounced in post-NCT PDAC. Simultaneous enrichment of the respiratory chain and depletion of glycolytic proteins such as GAPDH and LDHA, indicate a metabolic shift from Warburg effect back to mitochondrial energy supply in response to neoadjuvant therapy, which corroborates previous tissue and organoid PDAC studies.[28,34] Treatment-naïve and post-NCRT tumors show congruent expression patterns of complement components, which however contrasts previous gene expression studies of neoadjuvant treated PDAC.

In general, we noticed only poor differentiation of the type of neoadjuvant therapy applied in previous PDAC studies, illustrating the need for global proteome and transcriptome studies that characterize the PDAC biology in response to different types of neoadjuvant therapy.

We did not have access to treatment-naïve PDAC and healthy pancreas tissue from the same patients. However, we combined our data with the proteomic PDAC data of Werner et al and of the CPTAC. The three datasets displayed a large overlap of the identified proteins and a close relationship of the PDAC tissues. In future, combining proteomic data from various sources could yield broader insights into different disease conditions. Yet, our findings encourage deeper exploration of the biology of neoadjuvant treatment modalities in PDAC.

AUTHOR CONTRIBUTIONS

The study reported in the article has been performed by the authors, unless clearly specified in the text. All authors: conceptualization and writing—review & editing. Maren N. Stillger: methodology,

investigation, data curation, formal analysis, visualization, writing—original draft. Konrad Kurowski: investigation, methodology. Peter Bronsert: methodology, writing—original draft. Eva Brombacher: data curation, methodology. Clemens Kreutz: data curation, methodology. Martin Werner: funding acquisition, resources. Laura Tang: investigation, resources. Sylvia Timme-Bronsert: investigation, resources. Oliver Schilling: funding acquisition, methodology, resources, supervision, writing—original draft.

ACKNOWLEDGMENT

Open Access funding enabled and organized by Projekt DEAL.

FUNDING INFORMATION

The authors acknowledge funding by the Deutsche Forschungsgemeinschaft (DFG, projects 446058856, 466359513, 444936968, 405351425, 431336276, 43198400 [SFB 1453 "NephGen"], 441891347 [SFB 1479 "OncoEscape"], 423813989 [GRK 2606 "ProtPath"], 322977937 [GRK 2344 "MeInBio"]), the ERA PerMed program (BMBF, 01KU1916, 01KU1915A), the German Consortium for Translational Cancer Research (project Impro-Rec), the Matrix-Code research group, FRIAS, Freiburg, the investBW program BW1_1198/03 and the ERA TransCan program (project 01KT2201, "PREDICO"). This study was supported by the Mushett Family Foundation.

CONFLICT OF INTEREST STATEMENT

The authors have no conflict of interests to declare.

DATA AVAILABILITY STATEMENT

Human mass spectrometry-based proteomics data is available at the European Genome-phenome Archive (https://ega-archive.org) under the accession code: EGAD00010002388. The SRA files used for the proteogenomic analysis are listed in Table S2. Further information is available from the corresponding author upon request.

ETHICS STATEMENT

This study was performed in line with the principles of the Declaration of Helsinki and was approved by the Institutional Review Board of the Memorial Sloan Kettering Cancer Center, New York, USA. Informed consent was obtained from all individual participants included in the study.

ORCID

Maren N. Stillger https://orcid.org/0000-0001-6718-3911

REFERENCES

1. Siegel RL, Miller KD, Fuchs HE, Jemal A. Cancer statistics, 2021. *CA Cancer J Clin*. 2021;71(1):7-33.
2. Rahib L, Smith BD, Aizenberg R, Rosenzweig AB, Fleshman JM, Matrisian LM. Projecting cancer incidence and deaths to 2030: the unexpected burden of thyroid, liver, and pancreas cancers in the United States. *Cancer Res*. 2014;74(11):2913-2921.
3. Hackert T, Ulrich A, Büchler MW. Can neoadjuvant therapy in pancreatic cancer increase the Pool of patients eligible for pancreaticoduodenectomy? *Adv Surg*. 2017;51(1):1-10.
4. Klaiber U, Leonhardt CS, Strobel O, Tjaden C, Hackert T, Neoptolemos JP. Neoadjuvant and adjuvant chemotherapy in pancreatic cancer. *Langenbecks Arch Surg*. 2018;403(8):917-932.
5. Adamska A, Elaskalani O, Emmanouilidi A, et al. Molecular and cellular mechanisms of chemoresistance in pancreatic cancer. *Adv Biol Regul*. 2018;68:77-87.
6. Bittoni A, Santoni M, Lanese A, Pellei C, Andrikou K, Stefano C. Neoadjuvant therapy in pancreatic cancer: An emerging strategy. *Gastroenterol Res Pract*. 2014;2014:183852.
7. Chopra A, Hodges JC, Olson A, et al. Outcomes of neoadjuvant chemotherapy versus chemoradiation in localized pancreatic cancer: a case-control matched analysis. *Ann Surg Oncol*. 2021;28(7):3779-3788.
8. Gillen S, Schuster T, Meyer Zum Büschenfelde C, Friess H, Kleeff J. Preoperative/neoadjuvant therapy in pancreatic cancer: a systematic review and meta-analysis of response and resection percentages. *PLoS Med*. 2010;7(4):e1000267.
9. Townend P, de Reuver PR, Chua TC, et al. Histopathological tumour viability after neoadjuvant chemotherapy influences survival in resected pancreatic cancer: analysis of early outcome data. *ANZ J Surg*. 2018;88(3):E167-E172.
10. Sahni S, Nahm C, Krisp C, et al. Identification of novel biomarkers in pancreatic tumor tissue to predict response to neoadjuvant chemotherapy. *Front Oncol*. 2020;4(10):237.
11. O'Rourke MB, Sahni S, Samra J, Mittal A, Molloy MP. Data independent acquisition of plasma biomarkers of response to neoadjuvant chemotherapy in pancreatic ductal adenocarcinoma. *J Proteomics*. 2021;16(231):103998.
12. Amrutkar M, Verbeke CS, Finstadsveen AV, Dorg L, Labori KJ, Gladhaug IP. Neoadjuvant chemotherapy is associated with an altered metabolic profile and increased cancer stemness in patients with pancreatic ductal adenocarcinoma. *Mol Oncol*. 2022;17(1):1878-0261.13344.
13. Dias Costa A, Väyrynen SA, Chawla A, et al. Neoadjuvant chemotherapy is associated with altered immune cell infiltration and an anti-tumorigenic microenvironment in resected pancreatic cancer. *Clin Cancer Res*. 2022;28(23):5167-5179.
14. Werner J, Bernhard P, Cosenza-Contreras M, et al. Targeted and explorative profiling of kallikrein proteases and global proteome biology of pancreatic ductal adenocarcinoma, chronic pancreatitis, and normal pancreas highlights disease-specific proteome remodelling. *Neoplasia*. 2023;36:100871.
15. Sadot E, Doussot A, O'Reilly EM, et al. FOLFIRINOX induction therapy for Stage 3 pancreatic adenocarcinoma. *Ann Surg Oncol*. 2015;22(11):3512-3521.
16. Föll MC, Fahrner M, Oria VO, et al. Reproducible proteomics sample preparation for single FFPE tissue slices using acid-labile surfactant and direct trypsinization. *Clin Proteomics*. 2018;15(1):11.
17. Demichev V, Messner CB, Vernardis SI, Lilley KS, Ralser M. DIA-NN: neural networks and interference correction enable deep proteome coverage in high throughput. *Nat Methods*. 2020;17(1):41-44.
18. R Core Team. R: A Language and Environment for Statistical Computing [Internet]. Vienna, Austria: R Foundation for Statistical Computing. 2022 https://www.R-project.org/
19. Ellis MJ, Gillette M, Carr SA, et al. Connecting genomic alterations to cancer biology with proteomics: the NCI clinical proteomic tumor analysis consortium. *Cancer Discov*. 2013;3(10):1108-1112.
20. Johnson WE, Li C, Rabinovic A. Adjusting batch effects in microarray expression data using empirical Bayes methods. *Biostatistics*. 2007;8(1):118-127.
21. Egert J, Brombacher E, Warscheid B, Kreutz C. DIMA: data-driven selection of an imputation algorithm. *J Proteome Res*. 2021;20(7):3489-3496.
22. Hong SM, Goggins M, Wolfgang CL, et al. Vascular invasion in infiltrating ductal adenocarcinoma of the pancreas can mimic pancreatic

intraepithelial neoplasia: a histopathologic study of 209 cases. *Am J Surg Pathol*. 2012;36(2):235-241.
23. Karachaliou GS, Lazarou V, Giannis D, Astras G, Moris D, Petrou A. Initial experience with neoadjuvant FOLFIRINOX as first line therapy for locally advanced pancreatic cancer. *J BUON off J Balk Union Oncol*. 2020;25(5):2525-2527.
24. Itchins M, Arena J, Nahm CB, et al. Retrospective cohort analysis of neoadjuvant treatment and survival in resectable and borderline resectable pancreatic ductal adenocarcinoma in a high volume referral centre. *Eur J Surg Oncol J Eur Soc Surg Oncol Br Assoc Surg Oncol*. 2017;43(9):1711-1717.
25. Fröhlich K, Brombacher E, Fahrner M, et al. Benchmarking of analysis strategies for data-independent acquisition proteomics using a large-scale dataset comprising inter-patient heterogeneity. *Nat Commun*. 2022;13(1):2622.
26. Cao L, Huang C, Cui Zhou D, et al. Proteogenomic characterization of pancreatic ductal adenocarcinoma. *Cell*. 2021;184(19):5031-5052.e26.
27. Oria VO, Bronsert P, Thomsen AR, et al. Proteome profiling of primary pancreatic ductal adenocarcinomas undergoing additive chemoradiation link ALDH1A1 to early local recurrence and chemoradiation resistance. *Transl Oncol*. 2018;11(6):1307-1322.
28. Farshadi EA, Chang J, Sampadi B, et al. Organoids derived from neoadjuvant FOLFIRINOX patients recapitulate therapy resistance in pancreatic ductal adenocarcinoma. *Clin Cancer Res*. 2021;27(23):6602-6612.
29. Clark DW, Palle K. Aldehyde dehydrogenases in cancer stem cells: potential as therapeutic targets. *Ann Transl Med*. 2016;4(24):518.
30. Jamieson NB, Carter CR, McKay CJ, Oien KA. Tissue biomarkers for prognosis in pancreatic ductal adenocarcinoma: a systematic review and meta-analysis. *Clin Cancer Res*. 2011;17(10):3316-3331.
31. Ohuchida K, Mizumoto K, Miyasaka Y, et al. Over-expression of S100A2 in pancreatic cancer correlates with progression and poor prognosis. *J Pathol*. 2007;213(3):275-282.
32. Lin H, Yang P, Li B, et al. S100A10 promotes pancreatic ductal adenocarcinoma cells proliferation, migration and adhesion through JNK/-LAMB3-LAMC2 Axis. *Cancer*. 2022;15(1):202.
33. Wilson DN, Doudna Cate JH. The structure and function of the eukaryotic ribosome. *Cold Spring Harb Perspect Biol*. 2012;4(5):a011536.
34. McDonald OG. The biology of pancreatic cancer morphology. *Pathology (Phila)*. 2022;54(2):236-247.
35. Nakajima K, Ino Y, Naito C, et al. Neoadjuvant therapy alters the collagen architecture of pancreatic cancer tissue via ephrin-A5. *Br J Cancer*. 2022;126(4):628-639.
36. Dangi-Garimella S, Krantz SB, Barron MR, et al. Three-dimensional collagen I promotes gemcitabine resistance in pancreatic cancer through MT1-MMP-mediated expression of HMGA2. *Cancer Res*. 2011;71(3):1019-1028.
37. Iacobuzio-Donahue CA, Ryu B, Hruban RH, Kern SE. Exploring the host desmoplastic response to pancreatic carcinoma. *Am J Pathol*. 2002;160(1):91-99.
38. Zhou X, An J, Kurilov R, et al. Persister cell phenotypes contribute to poor patient outcomes after neoadjuvant chemotherapy in PDAC. *Nat Cancer*. 2023;4(9):1362-1381.
39. Mueller AC, Piper M, Goodspeed A, et al. Induction of ADAM10 by RT drives fibrosis, resistance, and EMT in pancreatic cancer. *Cancer Res*. 2021;81(12):3255-3269.
40. Farren MR, Sayegh L, Ware MB, et al. Immunologic alterations in the pancreatic cancer microenvironment of patients treated with neoadjuvant chemotherapy and radiotherapy. *JCI Insight*. 2020;5(1):130362.
41. Rutkowski MJ, Sughrue ME, Kane AJ, Mills SA, Parsa AT. Cancer and the complement cascade. *Mol Cancer Res MCR*. 2010;8(11):1453-1465.
42. Mamidi S, Höne S, Kirschfink M. The complement system in cancer: ambivalence between tumour destruction and promotion. *Immunobiology*. 2017;222(1):45-54.
43. Roumenina LT, Daugan MV, Petitprez F, Sautès-Fridman C, Fridman WH. Context-dependent roles of complement in cancer. *Nat Rev Cancer*. 2019;19(12):698-715.
44. Melmer A, Fineder L, Lamina C, et al. Plasma concentrations of the vitamin E-binding protein afamin are associated with overall and progression-free survival and platinum sensitivity in serous ovarian cancer: a study by the OVCAD consortium. *Gynecol Oncol*. 2013;128(1):38-43.
45. Humphries JM, Penno MAS, Weiland F, et al. Identification and validation of novel candidate protein biomarkers for the detection of human gastric cancer. *Biochim Biophys Acta BBA - Proteins Proteom*. 2014;1844(5):1051-1058.
46. de Freitas Chama LL, Ebstein F, Wiesrecker B, et al. Immunoproteasome impairment via β5i/LMP7-deletion leads to sustained pancreatic injury from experimental pancreatitis. *J Cell Mol Med*. 2021;25(14):6786-6799.
47. Dunn TA, Chen S, Faith DA, et al. A novel role of myosin VI in human prostate cancer. *Am J Pathol*. 2006;169(5):1843-1854.
48. Naora H, Montell DJ. Ovarian cancer metastasis: integrating insights from disparate model organisms. *Nat Rev Cancer*. 2005;5(5):355-366.
49. Droeser RA, Hirt C, Eppenberger-Castori S, et al. High myeloperoxidase positive cell infiltration in colorectal cancer is an independent favorable prognostic factor. *PLoS One*. 2013;8(5):e64814.
50. Zeindler J, Angehrn F, Droeser R, et al. Infiltration by myeloperoxidase-positive neutrophils is an independent prognostic factor in breast cancer. *Breast Cancer Res Treat*. 2019;177(3):581-589.

SUPPORTING INFORMATION

Additional supporting information can be found online in the Supporting Information section at the end of this article.

How to cite this article: Stillger MN, Kurowski K, Bronsert P, et al. Neoadjuvant chemo- or chemo-radiation-therapy of pancreatic ductal adenocarcinoma differentially shift ECM composition, complement activation, energy metabolism and ribosomal proteins of the residual tumor mass. *Int J Cancer*. 2024;154(12):2162-2175. doi:10.1002/ijc.34867